

# The feasibility of predicting ground reaction forces during running from a trunk accelerometry driven mass-spring-damper model

Niels J Nedergaard<sup>1,2</sup>, Jasper Verheul<sup>1</sup>, Barry Drust<sup>1</sup>, Terence Etchells<sup>3</sup>, Paulo Lisboa<sup>3</sup>, Mark A Robinson<sup>1</sup>, Jos Vanrenterghem<sup>Corresp. 1,2</sup>

<sup>1</sup> Research Institute for Sport and Exercise Sciences, Liverpool John Moores University, Liverpool, United Kingdom

<sup>2</sup> Department of Rehabilitation Sciences, Katholieke Universiteit Leuven, Leuven, Belgium

<sup>3</sup> School of Computing & Mathematical Sciences, Liverpool John Moores University, Liverpool, United Kingdom

Corresponding Author: Jos Vanrenterghem

Email address: jos.vanrenterghem@kuleuven.be

**Background.** Monitoring the external ground reaction forces (GRF) acting on the human body during running could help to understand how external loads influence tissue adaptation over time. Although mass-spring-damper (MSD) models have the potential to simulate the complex multi-segmental mechanics of the human body and predict GRF, these models currently require input from measured GRF limiting their application in field settings. Based on the hypothesis that the acceleration of the MSD-model's upper mass primarily represents the acceleration of the trunk segment, this paper explored the feasibility of using measured trunk accelerometry to estimate the MSD-model parameters required to predict GRF during running.

**Methods.** Twenty male athletes ran at approach speeds between 2 - 5 m·s<sup>-1</sup>. Resultant trunk accelerometry was used as a surrogate of the MSD-model upper mass acceleration to estimate the MSD-model parameters required to predict GRF. A purpose-built gradient descent optimisation routine was used where the MSD-model upper mass acceleration was fitted to the measured trunk accelerometer signal. Root mean squared errors (RMSE) were calculated to evaluate the accuracy of the trunk accelerometry fitting and GRF predictions. In addition, MSD-model parameters were estimated from fitting measured GRF, to explore the difference between model parameters estimated from trunk accelerometry and measured GRF.

**Results.** Despite a good match between the measured trunk accelerometry and the MSD-model's upper mass acceleration (median RMSE between 0.16 and 0.22 g), poor GRF predictions (median RMSE between 6.68 and 12.77 N·kg<sup>-1</sup>) were observed. In contrast, the MSD-model was able to replicate the measured GRF with high accuracy (median RMSE between 0.45 and 0.59 N·kg<sup>-1</sup>) across running speeds when model parameters were estimated from the measured GRF. The model parameters estimated from measured trunk accelerometry under- or overestimated the model parameters obtained from measured GRF, and generally demonstrated larger within parameter variations.

**Discussion.** Despite the potential of obtaining a close fit between the MSD-model's upper mass acceleration and the measured trunk accelerometry, the model parameters estimated from this process were inadequate to predict GRF waveforms during slow to moderate speed running. We therefore conclude that trunk-mounted accelerometry alone is inappropriate as input for the MSD-model to predict meaningful GRF waveforms. Further investigations are needed to continue to explore the feasibility of using body-worn micro sensor technology to drive simple human body models that would allow practitioners and researchers to estimate and monitor GRF waveforms in field settings.

1 **The feasibility of predicting ground reaction forces during**  
2 **running from a trunk accelerometry driven mass-spring-**  
3 **damper model**

4

5 Niels J Nedergaard<sup>1,2</sup>, Jasper Verheul<sup>1</sup>, Barry Drust<sup>1</sup>, Terence Etchells<sup>3</sup>, Paulo Lisboa<sup>3</sup>, Mark A Robinson<sup>1</sup>,  
6 Jos Vanrenterghem<sup>1,2</sup>

7 <sup>1</sup> Research Institute for Sport and Exercise Sciences, Liverpool John Moores University, Liverpool, United  
8 Kingdom

9 <sup>2</sup> Department of Rehabilitation Sciences, Katholieke Universiteit Leuven, Leuven, Belgium

10 <sup>3</sup> School of Computing & Mathematical Sciences, Liverpool John Moores University, Liverpool, United  
11 Kingdom

12

13 Corresponding Author:

14 Jos Vanrenterghem<sup>1,2</sup>

15 Tervuursevest 101 – box 1501, Leuven, 3001, Belgium

16 Email address: [jos.vanrenterghem@kuleuven.be](mailto:jos.vanrenterghem@kuleuven.be)

## 18 **Abstract**

19 **Background.** Monitoring the external ground reaction forces (GRF) acting on the human body  
20 during running could help to understand how external loads influence tissue adaptation over  
21 time. Although mass-spring-damper (MSD) models have the potential to simulate the complex  
22 multi-segmental mechanics of the human body and predict GRF, these models currently require  
23 input from measured GRF limiting their application in field settings. Based on the hypothesis  
24 that the acceleration of the MSD-model's upper mass primarily represents the acceleration of  
25 the trunk segment, this paper explored the feasibility of using measured trunk accelerometry to  
26 estimate the MSD-model parameters required to predict GRF during running.

27 **Methods.** Twenty male athletes ran at approach speeds between 2 - 5 m·s<sup>-1</sup>. Resultant trunk  
28 accelerometry was used as a surrogate of the MSD-model upper mass acceleration to estimate  
29 the MSD-model parameters required to predict GRF. A purpose-built gradient descent  
30 optimisation routine was used where the MSD-model upper mass acceleration was fitted to the  
31 measured trunk accelerometer signal. Root mean squared errors (RMSE) were calculated to  
32 evaluate the accuracy of the trunk accelerometry fitting and GRF predictions. In addition, MSD-  
33 model parameters were estimated from fitting measured GRF, to explore the difference  
34 between model parameters estimated from trunk accelerometry and measured GRF.

35 **Results.** Despite a good match between the measured trunk accelerometry and the MSD-  
36 model's upper mass acceleration (median RMSE between 0.16 and 0.22 g), poor GRF  
37 predictions (median RMSE between 6.68 and 12.77 N·kg<sup>-1</sup>) were observed. In contrast, the  
38 MSD-model was able to replicate the measured GRF with high accuracy (median RMSE between  
39 0.45 and 0.59 N·kg<sup>-1</sup>) across running speeds when model parameters were estimated from the

40 measured GRF. The model parameters estimated from measured trunk accelerometry under-  
41 or overestimated the model parameters obtained from measured GRF, and generally  
42 demonstrated larger within parameter variations.

43 **Discussion.** Despite the potential of obtaining a close fit between the MSD-model's upper mass  
44 acceleration and the measured trunk accelerometry, the model parameters estimated from this  
45 process were inadequate to predict GRF waveforms during slow to moderate speed running.  
46 We therefore conclude that trunk-mounted accelerometry alone is inappropriate as input for  
47 the MSD-model to predict meaningful GRF waveforms. Further investigations are needed to  
48 continue to explore the feasibility of using body-worn micro sensor technology to drive simple  
49 human body models that would allow practitioners and researchers to estimate and monitor  
50 GRF waveforms in field settings.

## 52 Introduction

53 Humans generate considerable forces against the ground during running to maintain an upright  
54 posture. This comes at the cost of equal and opposite ground reaction forces (GRF) acting on  
55 the body during every foot-ground contact (Cavanagh & LaFortune, 1980). These GRF put the  
56 body's soft tissues (e.g. bones, cartilage, muscles, tendons and ligaments) under biomechanical  
57 stresses which over time are expected to lead to beneficial structural adaptations (Kibler,  
58 Chandler & Stracener, 1992; Dye, 2005). Inadequate recovery or repetitive GRF with excessive  
59 magnitudes can instead lead to negative adaptations and tissue damage (Kibler, Chandler &  
60 Stracener, 1992; Dye, 2005). The ability to monitor an athlete's GRF during running can  
61 therefore help to better understand the relationship between the external forces experienced  
62 and soft-tissue adaptations (Vanrenterghem et al., 2017) ultimately helping to prevent  
63 musculoskeletal injury.

64

65 Monitoring GRF during running is currently restricted to laboratory environments where GRF  
66 are measured with force platforms built into the ground, or derived from whole-body  
67 kinematics (Bobbert, Schamhardt & Nigg, 1991; Winter, 2005). With recent developments of  
68 low-cost sensor based micro technology (Camomilla et al., 2018), accelerometry has become a  
69 popular tool to evaluate running mechanics outside laboratory environments in long and  
70 middle distance running (Tao et al., 2012) and professional team sports (Akenhead & Nassis,  
71 2016). Accelerometry also offers opportunities to estimate GRF, and tibia-mounted  
72 accelerometry has for example been used as surrogate measure of peak GRF since the early 90s  
73 (LaFortune, 1991; LaFortune, Lake & Hennig, 1995). However, recent studies found weak to

74 moderate linear relationships between peak accelerations measured from body-worn  
75 accelerometry (trunk- and tibia-mounted accelerometers) and peak whole-body accelerations  
76 measured from force platforms during running (Wundersitz et al., 2013; Nedergaard et al.,  
77 2017; Raper et al., 2018). Since body-worn accelerometers only measure segmental  
78 acceleration, the use of a single accelerometer is inadequate to incorporate the complex multi-  
79 segmental accelerations that result in specific GRF patterns (Nedergaard et al., 2017). Recent  
80 studies have indicated that from the combination of three or more body-worn inertial sensors  
81 and machine learning one can estimate GRF and knee joint moments with reasonable accuracy  
82 during running related locomotion (Johnson et al., 2018; Wouda et al., 2018), but the broader  
83 application of such approaches is constrained by the requirement of multiple sensors, machine  
84 learning tools, and large data sets. Therefore, if it were possible to estimate accurate GRF  
85 waveforms from a single body-worn sensor, it would provide practitioners and researchers with  
86 a useful tool to monitor the biomechanical load in field settings.

87

88 Since the overall motion of the human body has a spring-like behaviour during running, simple  
89 mass-spring models, consisting of a single mass and spring, have been widely used to estimate  
90 the vertical GRF in field settings (e.g. Alexander, 1984; Blickhan, 1989; McMahon & Cheng,  
91 1990). Moreover, such models have been used in combination with trunk-mounted  
92 accelerometry to estimate the required model parameters (Gaudino et al., 2013; Buchheit, Gray  
93 & Morin, 2015). Unfortunately, the initial high-frequency impact peak typically observed in the  
94 GRF waveform during running, which is speculated to be linked with negative tissue  
95 adaptations and risk of injury (Nigg, Cole & Bruggemann, 1995; Hreljac, Marshall & Hume, 2000;

96 Milner et al., 2006), cannot be estimated with this oversimplified model (Alexander, Bennett &  
97 Ker, 1986; Bullimore & Burn, 2007). A more complex mass-spring-damper model (MSD-model)  
98 better replicates the GRF waveforms for running, including both impact and active peaks  
99 (Derrick, Caldwell & Hamill, 2000). This model consists of a lower mass connected to a spring in  
100 parallel with a damper, representing the support leg during foot-ground contact, and an upper  
101 mass and spring representing the dynamics of the rest of the body. However, the ability to use  
102 trunk-mounted accelerometry to estimate the required model parameters for this model is yet  
103 unknown.

104

105 The aim of this study was to examine if the acceleration of the MSD-model's upper mass  
106 represents the acceleration of the trunk segment measured with trunk-mounted accelerometry  
107 during running. This hypothesis seems feasible, since the trunk segment represents half of the  
108 body mass (Dempster, 1955). If this provides a reasonable approximation, it might be feasible  
109 to estimate the required MSD-model parameters from trunk accelerometry to subsequently  
110 predict GRF from the MSD-model behaviour. Specifically, we therefore explored (1) the  
111 feasibility to estimate the MSD-model's eight natural model parameters from measured trunk  
112 accelerometry, and (2) whether these model parameters in fact predict reasonably accurate  
113 GRF waveforms during running at slow to moderate running speeds.

114

## 116 **Materials & Methods**

### 117 *Subjects and protocol*

118 Twenty healthy male athletes (age  $22 \pm 4$  years, height  $178 \pm 8$  cm, mass  $76 \pm 11$  kg) who  
119 engaged in running related sports activities on a weekly basis volunteered to participate in this  
120 study. The institutional ethics committee at Liverpool John Moores University granted ethical  
121 approval for this study (ethics approval number: 09/SPS/010) in accordance with the  
122 Declaration of Helsinki, and written consent was obtained from all participants. After a warm-  
123 up and an individual number of familiarisation trials the participants were asked to run over a  
124 force platform at different running speeds of 2, 3, 4 and  $5 \text{ m}\cdot\text{s}^{-1}$  ( $\pm 5\%$ ) in a randomised  
125 condition order. Running speeds were measured with photocell timing gates (Brower Timing  
126 System, Utah, USA) positioned 2 m apart and 2 m from the centre of the force platform as  
127 described in Vanrenterghem et al. (2012). The participants completed four trials of each  
128 running speed, landing on the force platform with their dominant leg.

129

### 130 *Experimental measurements*

131 Resultant ground reaction forces were measured (*GRF*) with a sampling frequency of 3000 Hz  
132 from a  $0.9 \times 0.6 \text{ m}^2$  Kistler force platform (9287C, Kistler Instruments Ltd., Winterthur,  
133 Switzerland). Resultant trunk accelerations (*TrunkAcc*) were simultaneously collected at 100 Hz  
134 using a tri-axial accelerometer (KXP94, Kionex, Inc., Ithaca, NY, USA) with an output range of  $\pm$   
135 13 g embedded within a commercial GPS device (MinimaxX S4, Catapult Innovations, Scoresby,  
136 Australia) with a total weight of 67 grams and  $88 \times 50 \times 19$  mm in dimension. The GPS device  
137 was positioned on the dorsal part of the upper trunk between the scapulae within a small

138 pocket of a tight fitted elastic vest according to the manufacturer's recommendations (Boyd,  
 139 Ball & Aughey, 2011). TrunkAcc and GRF were synchronised using a combination of time and  
 140 event synchronisation as described in Nedergaard et al. (2017) and exported to Matlab (version  
 141 R2016a, The MathWorks, Inc., Natick, MA, USA) where a 4<sup>th</sup> order recursive Butterworth low-  
 142 pass filter with a cut-off frequency of 20 Hz was applied to GRF and TrunkAcc. Only data from  
 143 the stance phase were collected, where touch down and take off were defined when the  
 144 vertical GRF crossed a 20 N threshold.

145

#### 146 *Mass-spring-damper model*

147 The complex multi-segmental dynamics of the human body during stance phase were modelled  
 148 as a passive MSD-model (Alexander, Bennett & Ker, 1986; Derrick, Caldwell & Hamill, 2000).  
 149 This model consists of two masses (Fig. 1); a lower point mass ( $m_2$ ) on top of a linear spring ( $k_2$ )  
 150 in parallel with a damper ( $c$ ) representing the support leg; an upper point mass ( $m_1$ )  
 151 representing the dynamics of the rest of the body and another linear spring ( $k_1$ ) connecting the  
 152 two masses.

153

154 The one-dimensional motion of the MSD-model was described by the acceleration of the two  
 155 masses (Eqn. 5 and 6):

156

$$157 \quad \lambda = \frac{m_1}{m_2} \tag{1}$$

$$158 \quad \omega_1^2 = \frac{k_1}{m_1} = \frac{(1 + \lambda)k_1}{\lambda M} \tag{2}$$

$$159 \quad \omega_2^2 = \frac{k_2}{m_2} = \frac{(1 + \lambda)k_2}{M} \tag{3}$$

$$160 \quad \zeta = \frac{c}{2\sqrt{k_2 m_2}} \quad (4)$$

$$161 \quad a_1 = -\omega_1^2(p_1 - p_2) + g \quad (5)$$

$$162 \quad a_2 = -\omega_2^2 p_2 + \omega_1^2 \lambda(p_1 - p_2) - 2\zeta\omega_2^2 v_2 + g \quad (6)$$

$$163 \quad GRF_{model} = \frac{M\omega_2}{1+\lambda}(\omega_2 p_2 + 2\zeta v_2) \quad (7)$$

164

165 where  $p_1, p_2, v_1, v_2, a_1,$  and  $a_2$  are the initial positions, velocities and, accelerations of the two  
 166 masses ( $m_1$  and  $m_2$ ), respectively;  $\lambda$  is the mass ratio of the lower mass relative to the total  
 167 body mass (Eqn. 1);  $\omega_1^2$  and  $\omega_2^2$  are the natural frequencies of the springs (Eqn. 2 and Eqn. 3)  
 168 based on the linear spring constants ( $k_1$  and  $k_2$ ) and the mass of the two masses ( $m_1$  and  $m_2$ );  $\zeta$   
 169 is the damping ratio of the damper (Eqn. 4); and  $g$  is the acceleration from gravitational  
 170 acceleration ( $-9.81 \text{ m}\cdot\text{s}^{-1}$ ). The GRF acting on the MSD-model is calculated as in Eqn. 7, where  $M$   
 171 is the sum of the two masses (i.e. total body mass):

172

### 173 *Model parameter estimation*

174 To estimate the eight model parameters ( $p_1, p_2, v_1, v_2, \omega_1^2, \omega_2^2, \zeta, \lambda$ ), we used gravity corrected  
 175 TrunkAcc from the stance phase as a surrogate of the MSD-model's upper mass acceleration  
 176 (Fig. 2A). For each trial, model parameters were optimised by fitting the MSD-model's upper  
 177 mass acceleration ( $a_1$ ) to the TrunkAcc signal. A purpose-built gradient descent optimisation  
 178 routine in Matlab was used, where the two second-order differential equations of the MSD-  
 179 model's motion (Eqn. 5 and 6) were transformed to four first-order differential equations and  
 180 solved numerically with a Runge Kutta 4<sup>th</sup> order method. Root mean squared error (RMSE)

181 between TrunkAcc and  $a_1$  were calculated for every iteration to determine the optimal model  
182 parameter combination that best fitted TrunkAcc for the individual trials. The model  
183 parameters estimated from the TrunkAcc fitting were then used to predict the GRF from Eqn. 7.  
184 Furthermore, to help understand differences in estimated model parameters and the predicted  
185 versus measured GRF, we also estimated the eight model parameters by fitting the MSD-model  
186 to the measured GRF (Fig. 2B), similar to the approach previously described by Derrick et al.  
187 (2000).

188

### 189 *Statistical analysis*

190 Measured and modelled GRF were normalised to the participants' mass. RMSE between  
191 TrunkAcc and  $a_1$ , and between measured GRF and predicted GRF, were calculated to evaluate  
192 the accuracy of the TrunkAcc fitting and the predicted GRF, respectively. RMSE median and  
193 interquartile range (25<sup>th</sup> to 75<sup>th</sup> percentile) were calculated to determine the variation in the  
194 model's accuracy within and across running speeds. Similarly, the median and interquartile  
195 range (25<sup>th</sup> to 75<sup>th</sup> percentile) of the estimated model parameters were calculated to explore  
196 the variation within and across running speeds for the model parameters estimated both from  
197 measured TrunkAcc and GRF.

198

## 200 Results

201 The first step was to estimate the required model parameters that fit the MSD-model's upper  
202 mass acceleration to the measured TrunkAcc signal. The MSD-model was able to fit the  
203 measured TrunkAcc with good accuracy across running speeds, though  $a_1$  systematically  
204 underestimated the magnitude of the first peak observed in the accelerometry signal (Fig. 3A).  
205 The median RMSE (interquartile range 25<sup>th</sup> to 75<sup>th</sup> percentile) of the TrunkAcc fitting increased  
206 from 0.16 (0.12; 0.22) g at the slowest running speed to between 0.21 (0.16; 0.26) g and 0.22  
207 (0.16; 0.30) g for three faster running speeds. Though similar median RMSE values were  
208 observed across the three fastest running speeds, the interquartile range increased with  
209 increased running speeds (Fig. 3A). Despite the good match between  $a_1$  and TrunkAcc, poor  
210 GRF predictions were observed across running speeds (Fig. 3B) and the median RMSE of the  
211 predicted GRF systematically increased with running speeds, from 6.68 (3.81; 15.30) N·kg<sup>-1</sup> at 2  
212 m·s<sup>-1</sup> to 12.77 (7.78; 27.22) N·kg<sup>-1</sup> at 5 m·s<sup>-1</sup>.

213

214 Since the TrunkAcc estimated parameters resulted in poor GRF predictions, we next estimated  
215 the model parameters by fitting the MSD-model to the measured GRF waveforms (Fig. 2B) to  
216 determine if there was any difference between the two sets of model parameters and to  
217 compare the upper mass acceleration to the measured TrunkAcc. The MSD-model was able to  
218 replicate the measured GRF with high accuracy when model parameters were estimated to  
219 directly fit the measured GRF (Fig. 4B). This was reflected in the low RMSE median and  
220 interquartile ranges observed across all running speeds (2 m·s<sup>-1</sup>: 0.45 (0.36; 0.60); 3 m·s<sup>-1</sup>: 0.47  
221 (0.37; 0.61); 4 m·s<sup>-1</sup>: 0.53 (0.39; 0.66); 5 m·s<sup>-1</sup>: 0.59 (0.46; 0.73); All Speeds: 0.51 (0.39; 0.64)

222  $\text{N}\cdot\text{kg}^{-1}$ ). However, the MSD-model's upper mass acceleration profiles then deviated  
223 considerably from the acceleration profiles measured with trunk accelerometry (Fig. 4A). The  
224 model parameters also differed considerably from those estimated from fitting measured  
225 TrunkAcc (Fig. 4C and 4D). Namely, the model parameters demonstrated smaller within  
226 parameter variation, which was especially evident for  $p_2$  and  $v_2$ . Also, lower  $v_1$  (median  
227 difference  $0.47 \text{ m}\cdot\text{s}^{-1}$ ) and higher  $v_2$  (median difference  $-1.73 \text{ m}\cdot\text{s}^{-1}$ ) values were observed across  
228 running speeds.

229

## 231 Discussion

232 This study illustrates that the MSD-model's upper mass acceleration could be fitted to the  
233 measured trunk accelerometry with high accuracy, but the model parameters estimated from  
234 this process did not lead to accurate predictions of GRF waveforms across a range of slow to  
235 moderate running speeds. Further analysis of the MSD-model behaviour when fitting to the  
236 measured GRF revealed a considerable discrepancy in model parameters compared to when  
237 fitting the MSD-model to measured trunk accelerometry signals. These results demonstrate  
238 that our initial hypothesis that the MSD-model's upper mass acceleration primarily represents  
239 the acceleration of the trunk was false.

240

### 241 *Model parameter estimation*

242 The eight model parameters are fundamental to calculating the GRF acting on the MSD-model,  
243 and though fitting TrunkAcc was successful, the model parameters estimated from this  
244 approach resulted in poor GRF predictions. Based on the equation of the upper mass  
245 acceleration (Eqn. 5) and the model parameters estimated from TrunkAcc, it seems that the  
246 MSD-model was able to fit the TrunkAcc by keeping the initial position of the upper mass ( $p_1$ )  
247 and lower mass ( $p_2$ ) low, and by keeping the spring stiffness of the upper spring ( $\omega_1^2$ ) low.

248 Whereas  $p_1$  has minor influence on the predicted GRF, the velocity of the upper mass at initial  
249 contact ( $v_1$ ) is indirectly influenced by changes in the initial upper mass position ( $v_1 = \dot{p}_1$ ).

250 Derrick et al. (2000) found that decreased  $v_1$  has a large impact on the duration of the stance  
251 phase and therefore could have contributed to the overestimation of foot-ground contact (Fig.  
252 3B). Similarly, the MSD-model decreased the spring stiffness of the upper spring ( $\omega_1^2$ ) to better

253 fit the two acceleration peaks typically observed in the TrunkAcc data, which has previously  
254 been shown to increase the duration of the stance phase (Derrick, Caldwell & Hamill, 2000).  
255 Furthermore, the MSD-model lowered the initial position of the lower mass ( $p_2$ ), which  
256 previously has been shown to both increase the GRF at touch down and decrease the  
257 magnitude of the impact peak (Derrick, Caldwell & Hamill, 2000). We therefore believe that the  
258 high GRF values observed in our GRF predictions at touch down (Fig. 3B) were primarily related  
259 to the lower initial position of the lower mass ( $p_2$ ) required to fit the upper mass acceleration to  
260 the TrunkAcc. Finally, the MSD-model also kept the damping ratio ( $\zeta$ ) low to better fit the  
261 magnitude of the two acceleration peaks in the TrunkAcc. Decreasing the damping ratio, has  
262 however previously been shown to increase the oscillation in the model's GRF (Alexander,  
263 Bennett & Ker, 1986; Derrick, Caldwell & Hamill, 2000), and may therefore explain why our GRF  
264 predictions to a large extent include oscillating characteristics (Fig. 3B).

265

266 The comparison between model parameters estimated from the TrunkAcc and parameters  
267 estimated from measured GRF, clearly demonstrates that the model is unsuitable for predicting  
268 GRF from TrunkAcc. A closer look at the model parameters estimated from measured GRF,  
269 showed that the median position and velocity of the lower mass ( $p_2$  and  $v_2$ ) was constant across  
270 running speeds and only varied marginally within running speeds (Fig. 2C). In addition, only  
271 small differences in median damping ratios ( $\zeta$ ) were observed between running speeds in this  
272 study ( $\zeta$  between 0.31 and 0.39 au). It was in fact kept constant ( $\zeta = 0.35$  au) in the study by  
273 Derrick et al. (2000). Based on these observations we explored the effect of keeping  $p_2$ ,  $v_2$ , and  $\zeta$   
274 constant for all trials (using the median parameter estimated from fitting GRF across running

275 speeds), and for the remaining five model parameters use the trial specific parameters  
276 estimated from fitting  $a_1$  to TrunkAcc to re-calculate the predicted GRF (Fig. S1). Whilst this  
277 decreased the variability of the GRF prediction (RMSE interquartile range) both within and  
278 across running speeds, only minor improvements were observed in the GRF prediction. This  
279 indicated that keeping selected model parameters constant would not substantially improve  
280 the GRF prediction in future studies. Furthermore, when selected model parameters were kept  
281 constant, the original interaction between the model parameters estimated from the TrunkAcc  
282 fitting was broken. In other words, such an approach is like solving a jigsaw with pieces from  
283 another jigsaw.

284

#### 285 *MSD-model hypothesis*

286 If the trunk accelerometry data accurately represents the model's upper mass acceleration one  
287 would at least expect that the model parameters related to the motion and stiffness of the  
288 upper mass and spring ( $\rho_1, v_1, \omega_1^2$ ) would be close to the model parameters estimated when  
289 fitting measured GRF. This was however not the case, and therefore naturally raises the  
290 questions as to whether the upper mass acceleration is equivalent to the acceleration  
291 measured from trunk accelerometry during running. The trunk accelerometry driven MSD-  
292 model approach introduced in this study is based on the hypothesis that the model's upper  
293 mass primarily represents the mass and motion of the trunk segment (Alexander, Bennett &  
294 Ker, 1986; Derrick, Caldwell & Hamill, 2000). Our results suggest however that this is not the  
295 case, and that independent accelerations of other body segments (e.g. the swing leg and arms)  
296 significantly contribute to the MSD-model's upper mass accelerations. We therefore conclude

297 that the primary model hypothesis for this study was false, and that trunk-mounted  
298 accelerometry alone is inappropriate as input for the MSD-model to predict meaningful GRF  
299 waveforms.

300

301 A high initial peak related to the attenuation of the shock impact from the foot's collision with  
302 the ground (Hamill, Derrick & Holt, 1995; Derrick, 2004) dominated the TrunkAcc signals across  
303 running speeds. In contrast, a higher second peak related to the COM displacement during the  
304 stance phase dominated the upper mass acceleration when the MSD-model was fitted to  
305 measured GRF. This raised the technical question as to whether the poor GRF predictions  
306 observed from the measured accelerometer signal were partly a consequence of an artificially  
307 high frequency of that initial peak and whether the application of lower filter cut-off  
308 frequencies (cut-off frequencies of 20 Hz in the present study) would improve GRF predictions.  
309 To explore this, trunk accelerometry data of 10 representative participants was low-pass  
310 filtered with cut-off frequencies of 15, 10 and 5 Hz (Fig. S2). Whilst low cut-off frequencies  
311 (especially 10 and 5 Hz) to a large extent successfully removed the initial high-frequency peak in  
312 the accelerometry signal, and the RMSE between TrunkAcc and upper mass acceleration  
313 decreased, it only had a minor influence on the RMSE of the predicted GRF across running  
314 speeds (Fig. S2). Therefore, accelerometry post-processing did not improve the GRF predictions  
315 from TrunkAcc. This suggests that the trunk accelerometry signal in itself was not the main  
316 reason for the poor GRF predictions, but rather an incorrect hypothesis that the MSD-model's  
317 upper mass acceleration primarily represents the acceleration of the trunk segment.

318

### 319 *Replicating GRF from measured GRF*

320 Although TrunkAcc was unsuccessful in predicting GRF during running with a simple MSD-  
321 model, the MSD-model could successfully replicate measured GRF during slow to moderate  
322 running speeds. In fact, the inclusion of all eight model parameters in our optimisation routine,  
323 compared to only optimising the spring constants of the upper and lower spring ( $k_1$  and  $k_2$ ) and  
324 the position of the lower mass ( $p_2$ ) (Derrick *et al.*, 2000) allowed us to replicate the measured  
325 GRF with higher accuracy. These findings illustrate that despite the MSD-model simplicity it has  
326 the ability to replicate and potentially predict GRF for a range of running speeds. Since the  
327 model parameters associated with the lower mass and spring are crucial to predict GRF (Eqn.  
328 7), this may open opportunities to use segmental kinematics and/or accelerometry from lower  
329 extremities to estimate model parameters. Recent studies have for example shown promising  
330 results in predicting GRF during sprinting, in high level sprinters, when contact and flight time,  
331 in combination with kinematics from the ankle were used as input for a two-mass model  
332 (Udofa, Ryan & Weyand, 2016; Clark, Ryan & Weyand, 2017). Future studies is however still  
333 need to explore the use of body-worn micro sensor technology to drive simple human body  
334 models and predict GRF waveforms for a range running speeds.

335

### 336 *Model limitations*

337 A limitation with the MSD-model and the associated model parameters is that multiple  
338 parameter combinations exist when fitting the MSD-model to measured GRF waveforms. Whilst  
339 it could be of interest to further explore the physical meaning of the individual model  
340 parameters and their interactions, this was not possible due to the existence of multiple model

341 parameter solutions. Secondly, the MSD-model is a one-dimensional model, and therefore only  
342 allows the magnitude of the GRF to be estimated. We decided to predict the magnitude of the  
343 resultant GRF in our study, considering that we wanted to estimate the overall external  
344 biomechanical loading on the body, however we accept that others may prefer to predict the  
345 magnitude of the vertical GRF only. Ultimately, we believe that it is important to recognise that  
346 the MSD-model approach omits any direction specific load variations across running speeds,  
347 and that these may well be relevant in how the musculoskeletal tissues are exposed to stresses.  
348 Finally, the MSD-model is a passive elastic model and therefore does not account for additional  
349 energy generated by the body's "active" structures (muscles). Whilst a more complex model  
350 could account for this (Zadpoor & Nikooyan, 2010; Nikooyan & Zadpoor, 2011), it is  
351 questionable if this would allow for better GRF predictions from TrunkAcc. The complexity of  
352 such model would probably also defeat the overall purpose of using a simple model that is still  
353 applicable in field settings.

354

## 355 **Conclusions**

356 In this study, we demonstrated that the upper mass acceleration of a simple MSD-model can be  
357 fitted to measured trunk accelerometry signals with high accuracy during running at various  
358 speeds, but that the ensuing model parameters do not deliver accurate predictions of GRF  
359 waveforms. Despite the convenient hypothesis that the MSD-model's upper mass acceleration  
360 primarily represents the acceleration of the trunk, our results showed that this hypothesis is  
361 violated too much to still predict meaningful GRF waveforms. Nevertheless, further studies  
362 should continue to explore the use of data from wearable micro sensor technology to drive

363 simple human body models that could allow us to estimate GRF waveforms in field settings.

364 This would allow researchers and practitioners to better monitor the external biomechanical

365 loads to which the human body is exposed during running locomotion, ultimately supporting a

366 general quest towards field-based monitoring of tissue load-adaptation processes.

367

### 368 **Acknowledgements**

369 The authors would like to thank Ms Elena Eusterwiemann for her assistance with the data

370 collection.

372 **References**

- 373 Akenhead R., Nassis GP. 2016. Training Load and Player Monitoring in High-Level Football:  
374 Current Practice and Perceptions. *International Journal of Sports Physiology and*  
375 *Performance* 11:587–593. DOI: 10.1123/ijsp.2015-0331.
- 376 Alexander RM. 1984. Elastic Energy Stores in Running Vertebrates. *American Zoologist* 24:85–  
377 94. DOI: 10.1093/icb/24.1.85.
- 378 Alexander RM., Bennett MB., Ker RF. 1986. Mechanical properties and function of the paw pads  
379 of some mammals. *Journal of Zoology* 209:405–419. DOI: 10.1111/j.1469-  
380 7998.1986.tb03601.x.
- 381 Blickhan R. 1989. The spring-mass model for running and hopping. *Journal of Biomechanics*  
382 22:1217–1227. DOI: 10.1016/0021-9290(89)90224-8.
- 383 Bobbert MF., Schamhardt HC., Nigg BM. 1991. Calculation of vertical ground reaction force  
384 estimates during running from positional data. *Journal of Biomechanics* 24:1095–1105.  
385 DOI: 10.1016/0021-9290(91)90002-5.
- 386 Boyd LJ., Ball K., Aughey RJ. 2011. The Reliability of MinimaxX Accelerometers for Measuring  
387 Physical Activity in Australian Football. *International Journal of Sports Physiology and*  
388 *Performance* 6:311–321. DOI: 10.1123/ijsp.6.3.311.
- 389 Buchheit M., Gray AJ., Morin JB. 2015. Assessing Stride Variables and Vertical Stiffness with  
390 GPS-Embedded Accelerometers: Preliminary Insights for the Monitoring of Neuromuscular  
391 Fatigue on the Field. *Journal of Sports Science and Medicine* 14:698–701.
- 392 Bullimore SR., Burn JF. 2007. Ability of the planar spring-mass model to predict mechanical  
393 parameters in running humans. *J Theor Biol* 248:686–695. DOI: 10.1016/j.jtbi.2007.06.004.

- 394 Camomilla V., Bergamini E., Fantozzi S., Vannozzi G. 2018. Trends Supporting the In-Field Use of  
395 Wearable Inertial Sensors for Sport Performance Evaluation: A Systematic Review. *Sensors*  
396 18:873. DOI: 10.3390/s18030873.
- 397 Cavanagh PR., Lafortune MA. 1980. Ground reaction forces in distance running. *Journal of*  
398 *Biomechanics* 13:397–406. DOI: [http://dx.doi.org/10.1016/0021-9290\(80\)90033-0](http://dx.doi.org/10.1016/0021-9290(80)90033-0).
- 399 Clark KP., Ryan LJ., Weyand PG. 2017. A general relationship links gait mechanics and running  
400 ground reaction forces. *The Journal of Experimental Biology* 220:247–258. DOI:  
401 10.1242/jeb.138057.
- 402 Dempster WT. 1955. Space requirements of the seated operator: geometrical, kinematic, and  
403 mechanical aspects of the body with special reference to the limbs. Wright-Patterson Air  
404 Force Base, Ohio: Wright Air Development Center.
- 405 Derrick TR. 2004. The effects of knee contact angle on impact forces and accelerations. *Med Sci*  
406 *Sports Exerc* 36:832–837. DOI: 10.1249/01.MSS.0000126779.65353.CB.
- 407 Derrick TR., Caldwell GE., Hamill J. 2000. Modeling the stiffness characteristics of the human  
408 body while running with various stride lengths. *Journal of Applied Biomechanics* 16:36–51.  
409 DOI: 10.1123/jab.16.1.36.
- 410 Dye SF. 2005. The pathophysiology of patellofemoral pain: a tissue homeostasis perspective.  
411 *Clin Orthop Relat Res* 436:100–110. DOI: 10.1097/01.blo.0000172303.74414.7d.
- 412 Gaudino P., Gaudino C., Alberti G., Minetti AE. 2013. Biomechanics and predicted energetics of  
413 sprinting on sand: hints for soccer training. *J Sci Med Sport* 16:271–275. DOI:  
414 10.1016/j.jsams.2012.07.003.
- 415 Hamill J., Derrick TR., Holt KG. 1995. Shock attenuation and stride frequency during running.

- 416 *Human Movement Science* 14:45–60. DOI: <http://dx.doi.org/10.1016/0167->  
417 9457(95)00004-C.
- 418 Hreljac A., Marshall RN., Hume PA. 2000. Evaluation of lower extremity overuse injury potential  
419 in runners. *Med Sci Sports Exerc* 32:1635–1641.
- 420 Johnson WR., Mian A., Donnelly CJ., Lloyd D., Alderson J. 2018. Predicting athlete ground  
421 reaction forces and moments from motion capture. *Med Biol Eng Comput.* DOI:  
422 [doi.org/10.1007/s11517-018-1802-7](https://doi.org/10.1007/s11517-018-1802-7).
- 423 Kibler WB., Chandler TJ., Stracener ES. 1992. Musculoskeletal adaptations and injuries due to  
424 overtraining. *Exerc Sport Sci Rev* 20:99–126.
- 425 Lafortune MA. 1991. Three-dimensional acceleration of the tibia during walking and running.  
426 *Journal of Biomechanics* 24:877–886. DOI: 10.1016/0021-9290(91)90166-K.
- 427 Lafortune MA., Lake MJ., Hennig E. 1995. Transfer function between tibial acceleration and  
428 ground reaction force. *Journal of Biomechanics* 28:113–117. DOI: 10.1016/0021-  
429 9290(95)80014-X.
- 430 McMahon TA., Cheng GC. 1990. The mechanics of running: How does stiffness couple with  
431 speed? *Journal of Biomechanics* 23, Supple:65–78. DOI: <http://dx.doi.org/10.1016/0021->  
432 9290(90)90042-2.
- 433 Milner CE., Ferber R., Pollard CD., Hamill J., Davis IS. 2006. Biomechanical factors associated  
434 with tibial stress fracture in female runners. *Med Sci Sports Exerc* 38:323–328. DOI:  
435 10.1249/01.mss.0000183477.75808.92.
- 436 Nedergaard NJ., Robinson MA., Eusterwiemann E., Drust B., Lisboa PJ., Vanrenterghem J. 2017.  
437 The Relationship Between Whole-Body External Loading and Body-Worn Accelerometry

- 438 During Team-Sport Movements. *International Journal of Sports Physiology and*  
439 *Performance* 12:18–26. DOI: 10.1123/ijsp.2015-0712.
- 440 Nigg BM., Cole GK., Bruggemann GP. 1995. Impact forces during heel-toe running. *Journal of*  
441 *Applied Biomechanics* 11:407–432. DOI: 10.1123/jab.11.4.407.
- 442 Nikooyan AA., Zadpoor AA. 2011. An improved cost function for modeling of muscle activity  
443 during running. *J Biomech* 44:984–987. DOI: 10.1016/j.jbiomech.2010.11.032.
- 444 Raper DP., Witchalls J., Philips EJ., Knight E., Drew MK., Waddington G. 2018. Use of a tibial  
445 accelerometer to measure ground reaction force in running: A reliability and validity  
446 comparison with force plates. *Journal of Science and Medicine in Sport* 21:84–88. DOI:  
447 10.1016/j.jsams.2017.06.010.
- 448 Tao W., Liu T., Zheng R., Feng H. 2012. Gait analysis using wearable sensors. *Sensors* 12:2255–  
449 2283. DOI: 10.3390/s120202255.
- 450 Udofa AB., Ryan LJ., Weyand PG. 2016. Impact forces during running: Loaded questions,  
451 sensible outcomes. In: *2016 IEEE 13th International Conference on Wearable and*  
452 *Implantable Body Sensor Networks (BSN)*. 371–376. DOI: 10.1109/BSN.2016.7516290.
- 453 Vanrenterghem J., Nedergaard NJ., Robinson MA., Drust B. 2017. Training Load Monitoring in  
454 Team Sports: A Novel Framework Separating Physiological and Biomechanical Load-  
455 Adaptation Pathways. *Sports medicine (Auckland, N.Z.)*. DOI: 10.1007/s40279-017-0714-2.
- 456 Vanrenterghem J., Venables E., Pataky T., Robinson MA. 2012. The effect of running speed on  
457 knee mechanical loading in females during side cutting. *Journal of Biomechanics* 45:2444–  
458 2449. DOI: 10.1016/j.jbiomech.2012.06.029.
- 459 Winter DA. 2005. *Biomechanics and motor control of human movement*. Hoboken, N.J.: John

460 Wiley & Sons. DOI: 10.1002/9780470549148.

461 Wouda FJ., Giuberti M., Bellusci G., Maartens E., Reenalda J., van Beijnum B-JF., Veltink PH.

462 2018. Estimation of Vertical Ground Reaction Forces and Sagittal Knee Kinematics During

463 Running Using Three Inertial Sensors. *Frontiers in Physiology* 9:1–14. DOI:

464 10.3389/fphys.2018.00218.

465 Wundersitz DW., Netto KJ., Aisbett B., Gustin PB. 2013. Validity of an upper-body-mounted

466 accelerometer to measure peak vertical and resultant force during running and change-of-

467 direction tasks. *Sports Biomech* 12:403–412. DOI: 10.1080/14763141.2013.811284.

468 Zadpoor AA., Nikooyan AA. 2010. Modeling muscle activity to study the effects of footwear on

469 the impact forces and vibrations of the human body during running. *Journal of*

470 *Biomechanics* 43:186–193. DOI: 10.1016/j.jbiomech.2009.09.028.

471

# Figure 1

An illustration of the human body represented as a MSD-model.

The MSD-model consists of a lower mass spring damper element ( $m_2, k_2, c$ ) representing the support leg of the human body and an upper mass spring element ( $m_1, k_1$ ) representing the rest of the human body.

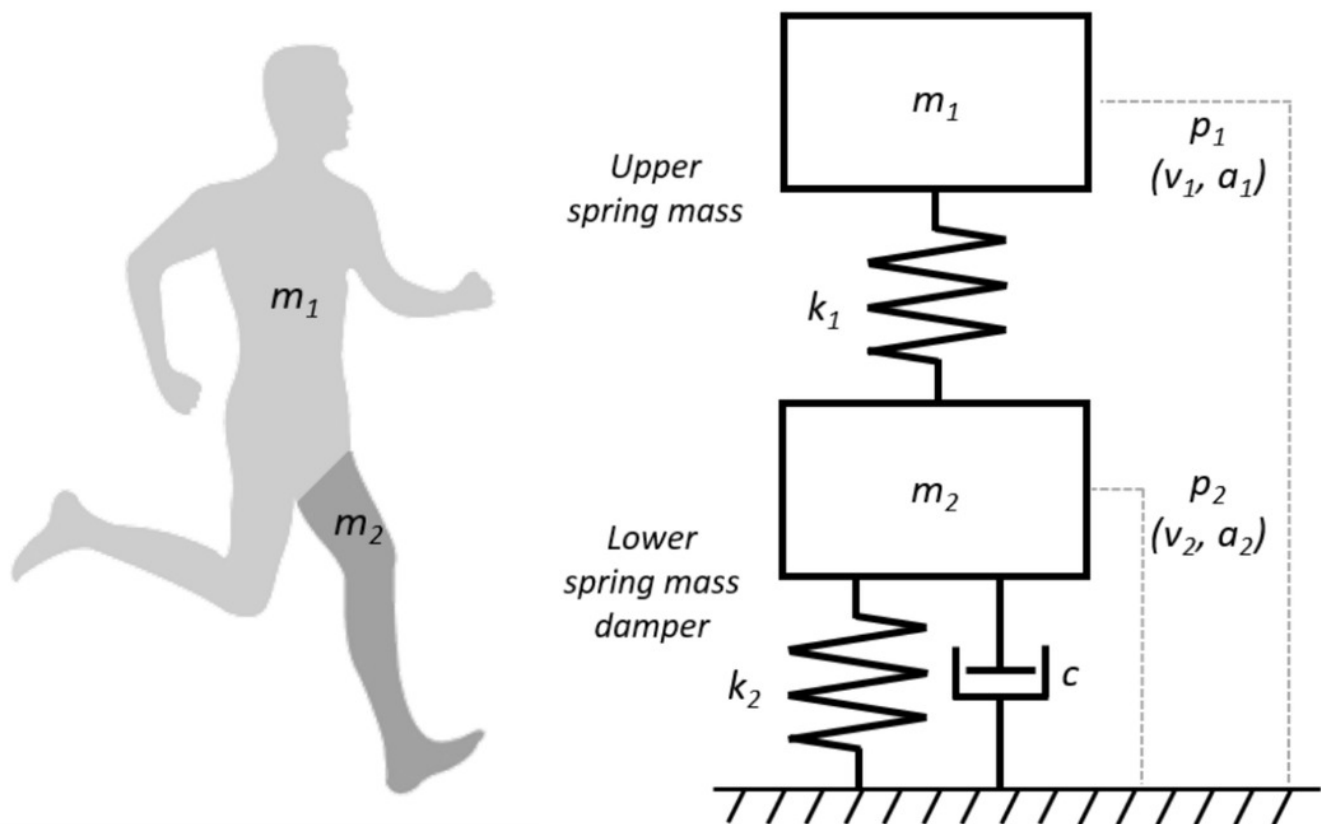


## Figure 2

Estimating MSD-model parameters by fitting the MSD-model to measured trunk accelerometry and measured GRF.

The top panel (A) illustrates the trunk driven MSD-model where measured trunk accelerometry (TrunkAcc) for the stance phase, is used to estimate the eight model parameters, based on the hypothesis that the MSD-model's upper mass acceleration ( $a_1$ ) primarily represents TrunkAcc, before GRF is calculated from the model parameter combination that best fitted TrunkAcc. The bottom panel (B) displays the traditional MSD-model approach, where the eight model parameters are estimated by fitting the model's GRF to the measured GRF.

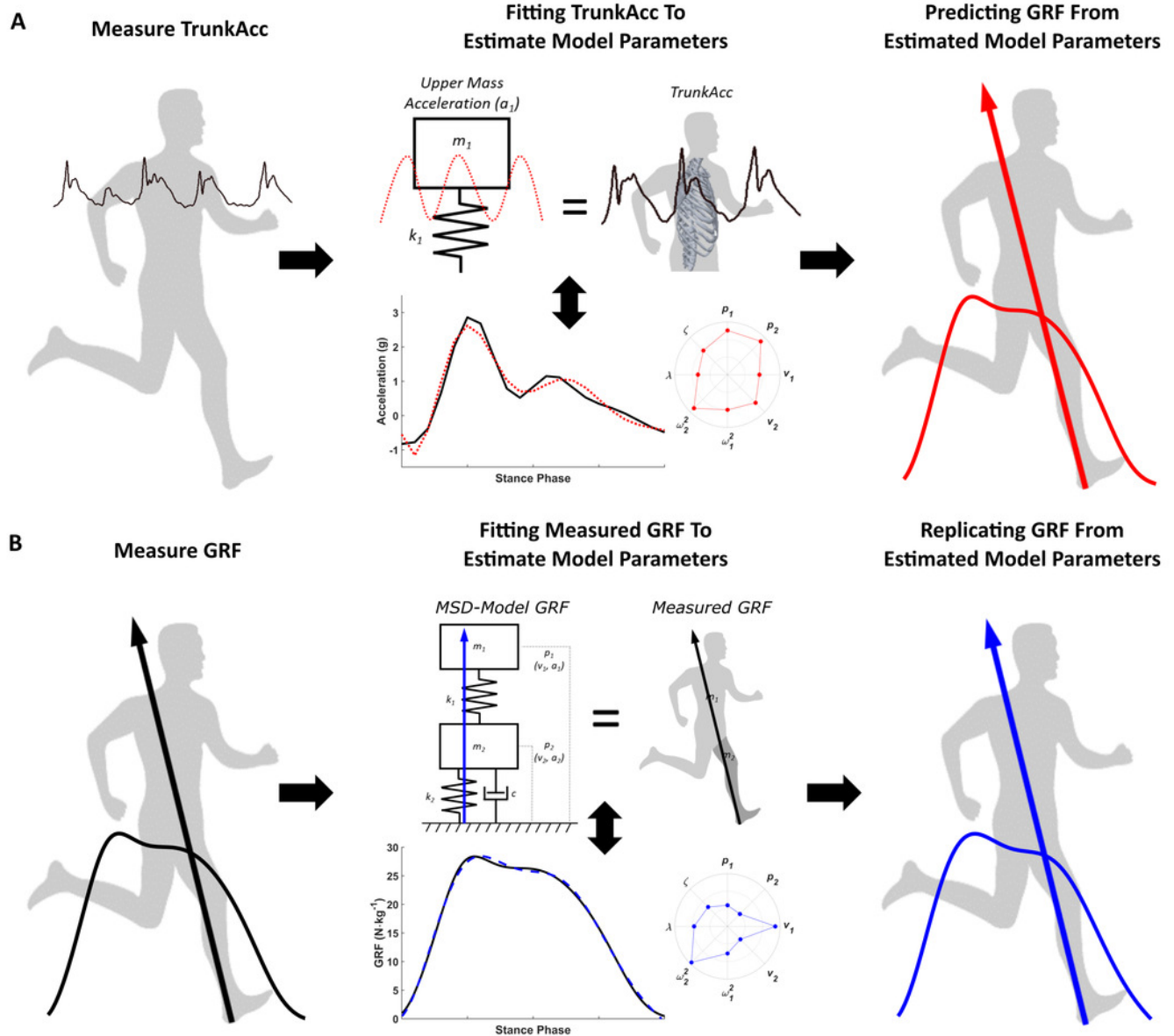


## Figure 3

Representative examples of the trunk accelerometry fitting and GRF prediction, and the median RMSE across running speeds.

Representative examples of fitting the upper mass acceleration to the trunk accelerometry signal across running speeds (A), and the measured and predicted GRF for the same trials (B). The RMSE for the trunk accelerometry fitting and GRF predictions are displayed in brackets for the individual examples. The boxplots on the right side display the RMSE median, and 25<sup>th</sup> and 75<sup>th</sup> interquartile range for the trunk accelerometry fitting and GRF prediction respectively across running speeds. Extreme outliers were removed from the boxplots.

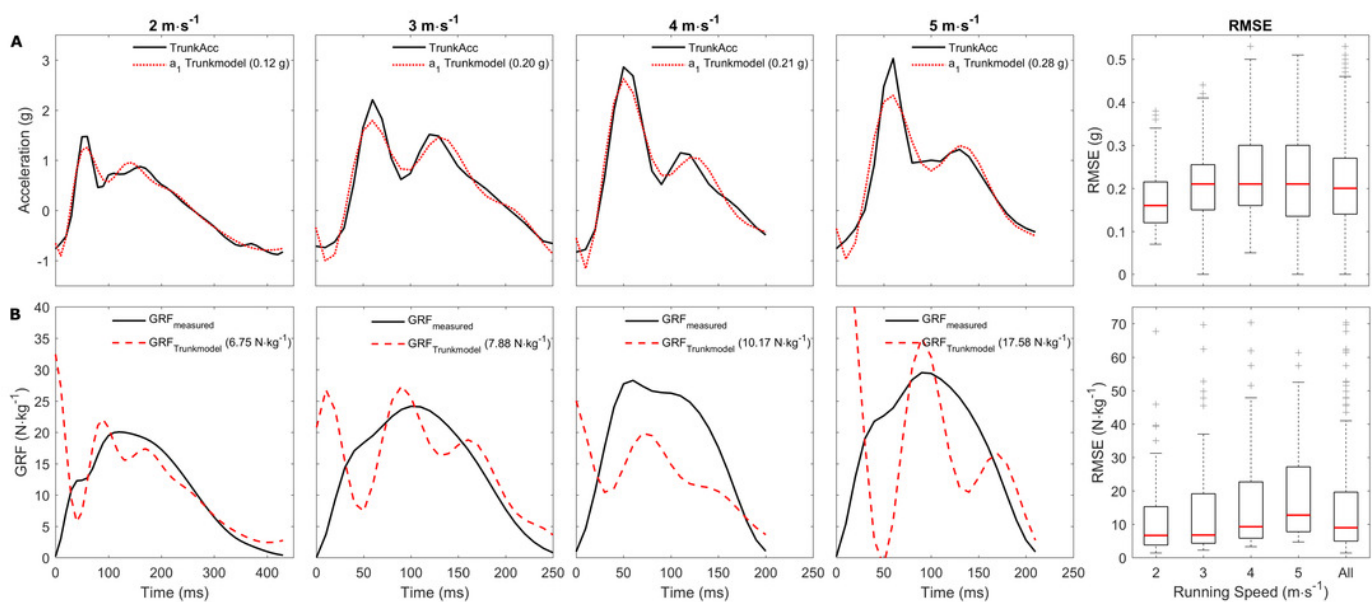


## Figure 4

Representative examples of the upper mass acceleration, GRF and median model parameters from the TrunkAcc and GRF fitting.

Representative examples of the measured trunk accelerometry and the MSD-model's upper mass acceleration (A), and the measured, predicted and replicated GRF (B). The RMSE for the trunk accelerometry fitting and GRF predictions are displayed in the brackets for the individual examples. The inserted polar plots display the estimated model parameters (in unscaled values) from the two approaches for the representative examples. The bottom two panels (C and D) display the median, 25<sup>th</sup> and 75<sup>th</sup> interquartile range for the model parameters estimated from measured trunk accelerometry and GRF respectively across running speeds. Extreme outliers were removed from the boxplots.

